European Journal of Radiology 120 (2019) 108667

Contents lists available at ScienceDirect

European Journal of Radiology

journal homepage: www.elsevier.com/locate/ejrad

Compressed SENSE accelerated 3D T1w black blood turbo spin echo versus 2D T1w turbo spin echo sequence in pituitary magnetic resonance imaging

Thomas Sartoretti[a,1], Elisabeth Sartoretti[a,1], Michael Wyss[a,b], Árpád Schwenk[a], Luuk van Smoorenburg[a], Barbara Eichenberger[a], Arash Najafi[a], Christoph Binkert[a], Anton S. Becker[c,d], Sabine Sartoretti-Schefer[a,*]

[a] Institute of Radiology, Kantonsspital Winterthur, Brauerstrasse 15, 8401, Winterthur, Switzerland
[b] Philips Healthsystems, Zürich, Switzerland
[c] Institute of Diagnostic and Interventional Radiology, University Hospital Zürich, University of Zürich, Raemistrasse 100, CH-8091, Zürich, Switzerland
[d] Department of Radiology, Memorial Sloan Kettering Cancer Center, New York, New York, USA

ARTICLE INFO

Keywords:
Pituitary gland
Magnetic resonance imaging
Diagnostic techniques and procedures

ABSTRACT

Purpose: To compare image quality between a 2D T1w turbo spin echo (TSE) sequence and a Compressed SENSE accelerated 3D T1w black blood TSE sequence (equipped with a black blood prepulse for blood signal suppression) in pre- and postcontrast imaging of the pituitary and to assess scan time reductions.

Methods and Materials: For this retrospective study, 56 patients underwent pituitary MR imaging at 3T. 28 patients were scanned with the 2D- and 28 patients with the accelerated 3D sequence. Two board certified neuroradiologists independently evaluated 13 qualitative image features (12 features on postcontrast- and 1 feature on precontrast images).SNR and CNR measurements were obtained. Interreader agreement was assessed with the intraclass correlation coefficient while differences in scores were assessed with exact Wilcoxon rank sum tests.

Results: The interreader agreement ranged from fair (visibility of the ophthalmic nerve, ICC = 0.57) to excellent (presence and severity of pulsation artefacts, ICC = 0.97). The Compressed SENSE accelerated 3D sequence outperformed the 2D sequence in terms of "overall image quality" (median: 4 versus 3, $p = 0.04$) and "presence and severity of pulsation artefacts" (median: 0 versus 1, $p < 0.001$). There were no significant differences in any other qualitative and quantitative (SNR, CNR) image quality features. Scan time was reduced by 03:53 min (33.1%) by replacing the 2D with the 3D sequence.

Conclusion: The Compressed SENSE accelerated 3D T1w black blood TSE sequence is a reliable alternative for the standard 2D sequence in pituitary imaging. The black blood prepulse may aid in suppression of pulsation artefacts.

1. Introduction

MR imaging (MRI) has emerged as the modality of choice for standard diagnostic imaging of pituitary lesions [1]. Especially 2D pre- and postcontrast T1-weighted(w) conventional spin echo (SE) or fast / turbo spin echo (FSE or TSE) as well as 3D gradient echo (GRE) and fast spin echo (FSE) sequences play an important role in evaluating lesions in the sella and the surrounding structures of cavernous sinus and orbits [1]. However, while 3D sequences are desirable as they enable superior soft tissue contrast, improved spatial resolution in the acquired images and may decrease partial volume effects, there are some drawbacks: 3D T1w GRE sequences have the disadvantage of susceptibility artefacts and high signal intensity from blood flow, which make image interpretation of contrast enhancing T1 hyperintense lesions in the

Abbreviations: MRI, MR imaging; SE, spin echo; FSE, fast spin echo; TSE, turbo spin echo gregradient echo; MSDE, motion-sensitized driven-equilibrium; ADA, anti-driven equilibrium; SNR, signal to noise ratio; CNR, contrast to noise ratio; ROI, region of interest; SI, signal intensity; SD, standard deviation; ICC, intraclass correlation coefficient; DIR, double inversion recovery; FLAIR, fluid-attenuated inversion recovery; TOF, time of flight; TFE, turbo field echo

* Corresponding author.
E-mail addresses: thomas.sartoretti@uzh.ch (T. Sartoretti), elisabeth.sartoretti@uzh.ch (E. Sartoretti), michael.wyss@ksw.ch (M. Wyss), arpad.schwenk@ksw.ch (Á. Schwenk), hendricus.vansmoorenburg@ksw.ch (L. van Smoorenburg), barbara.eichenberger@ksw.ch (B. Eichenberger), arash.najafi@ksw.ch (A. Najafi), christoph.binkert@ksw.ch (C. Binkert), anton.becker@usz.ch (A.S. Becker), sabine.sartoretti@ksw.ch (S. Sartoretti-Schefer).
[1] These authors contributed equally.

https://doi.org/10.1016/j.ejrad.2019.108667
Received 11 June 2019; Received in revised form 23 August 2019; Accepted 8 September 2019

cavernous sinus difficult [1–3]. 3D T1w TSE sequences, on the other hand, suffer from long scan times [1,3]. Thus, 2D T1w TSE images are still widely used in clinical routine. At our own institution, we also utilized four pre- and postcontrast 2D TSE T1w sequences in coronal and sagittal orientation and a dynamic coronal 2D GRE T1w sequence, all with 2 mm slice thickness, as part of the dedicated pituitary protocol. While a 2 mm slice thickness is generally too thick for the often very small pituitary lesions, a higher resolution would be even more time-consuming and thus hardly tolerable for the patient.

Following the introduction of compressed sensing MRI acceleration techniques, such as Compressed SENSE [4–6], our pituitary MRI protocol could be adjusted, thus enabling the implementation of new sequences without prolonging scan times.

Specifically, the 2D T1w TSE sequences (pre- and postcontrast) in coronal and sagittal plane of section were replaced by an accelerated isotropic transverse 3D T1w black blood TSE sequence (a black blood prepulse for blood signal suppression was added [7,8]) both for pre- and postcontrast imaging that allowed for secondary multiplanar reconstructions in sagittal and coronal image plane in the submillimeter range. Compressed SENSE is a combination of the parallel imaging technique SENSE (sensitivity encoding) together with compressed sensing. Both these techniques allow for a reduction of the amount of acquired k-space data (space from where MRI data is collected) therefore enabling an acceleration of MRI acquisitions. While MR imaging is in high demand, it is a time-consuming imaging technique, and thus the shortening of acquisition times preferably without a loss of image quality is of great interest to both patients and clinical institutions [5].

In SENSE-based acceleration, uniform undersampling strategies in the k-space domain are applied to reduce the amount of data sampled. Information from the different receive coil elements is used to create an image from the subsampled data. While the maximum SENSE acceleration factor is limited by the coil geometry, compressed sensing overcomes this limitation by allowing incoherent subsampling schemes in the k-space domain thus allowing for a further reduction of data sampled. This compressed sensing scheme results in structured noise patterns that can be removed by transforming these images to a domain in which they may be sparsely represented, such as a wavelet domain. In this domain, sparse information from the relevant structures in the images can easily be separated from the noise (so called denoising). In the Compressed SENSE implementation a variable density subsampling scheme was combined with a reconstruction algorithm that allows the combination of wavelet transformation of compressed sensing with coil information of SENSE [4–6].

While compressed sensing technology has been shown to be of great value to clinical institutions [5] to date no systematic evaluation of the clinical feasibility of a 3D T1w black blood TSE sequence for pituitary imaging accelerated with compressed sensing technology has been conducted. Thus, we compared the image quality between the 2D T1w TSE sequence and the accelerated 3D T1w black blood TSE sequence by comparing qualitative and quantitative image quality metrics and we also reviewed the scan time reduction resulting from replacing the 2D sequence with the 3D sequence.

2. Materials and methods

2.1. Patients

In this retrospective study 56 patients were selected, who underwent pituitary MR imaging at 3T.

28 patients, 13 males and 15 females with a mean age of 45.2 years (range 18 to 80 years) with clinically suspected sellar lesions [1] were examined before the implementation of the Compressed SENSE technique in the time from April 2016 to June 2018. Final diagnoses were macroadenoma in 9, microadenoma in 5, inflammatory process in cavernous sinus (i.e. Tolosa Hunt syndrome) in 1, Langerhans cell histiocytosis in 1, hypophysitis in 2 and normal pituitary imaging in 10 patients.

28 patients, 14 males and 14 females with a mean age of 45.3 years (range 18–77 years) with clinically suspected sellar lesions [1] were examined after the implementation of the Compressed SENSE technique with the new revised pituitary protocol in the time from June 2018 to April 2019. The final diagnoses were macroadenoma in 7, microadenoma in 5, inflammatory process in cavernous sinus (i.e. Tolosa Hunt syndrome) in 2, hypophysitis in 1, Langerhans cell histiocytosis in 1 and normal pituitary imaging in 12 patients.

This study was approved by the cantonal ethical committee with BASEC Number 2018-01275. Written informed consent was obtained from all subjects in this study.

2.2. MR imaging

Patients were examined on a 3T MR scanner (Philips Achieva, Best, the Netherlands).

The original MR protocol for pituitary imaging consisted of 2D T1w coronal and sagittal pre- and postcontrast TSE sequences, of a 2D T2w coronal TSE sequence and of a 2D T1w coronal dynamic GRE sequence.

The revised MR protocol after implementation of Compressed SENSE consisted of an accelerated isotropic pre- and postcontrast 3D T1w black blood TSE sequence (Compressed SENSE factor 3.1), acquired in transverse plane of section, and of an accelerated isotropic 3D T2w TSE DRIVE sequence (Compressed SENSE factor 2.8), acquired in sagittal plane of section. The 2D T1w coronal dynamic GRE sequence was added to the protocol without any changes. Imaging parameters of the 2D T1w and 2D T2w coronal and sagittal pre- and postcontrast TSE sequence as well as of the accelerated 3D T1w black blood TSE pre- and postcontrast transverse MR sequence, the accelerated 3D T2w TSE

Table 1
MR parameters of the T1w sequences.

	3D T1w black blood TSE pre- and postcontrast	2D T1w coronal TSE pre- and postcontrast	2D T1w sagittal TSE pre- and postcontrast
FOV	230 × 200 x 70 mm	180 × 180 × 38	150 x 150 mm
Acquisition voxel	0.75 × 0.75 x 0.75 mm	0.62 × 0.78 x 2.0 mm	0.6 × 0.65 x 2.0 mm
Reconstruction voxel	0.4 × 0.4 x 0.4 mm	0.28 × 0.28 x 2.0 mm	0.47 × 0.47 x 2.0 mm
Number of slices	187	19	12
Slice thickness, gap	0.75 mm −0.4 mm	2.0 mm, 0.2 mm	2.0 mm, 0.2 mm
Compressed SENSE factor	CS 3.1	no	no
Scan mode	3D	2D	2D
TSE factor	40	5	5
Flip angle (in degrees)	90	90	90
TR,TE, TE equivalent	TR 600 ms TE 32 ms/26 ms	TR 735 ms TE 7.4 ms	TR 675 ms TE 7.9 ms
Fat suppression	SPIR	no	no
Number of acquisitions	2	2.6	2
Receiver bandwidth	598 Hz/pixel	239 Hz/pixel	260 Hz / pixel
Scan duration	04:35 min	03:11 min	03:40 min

Table 2
: MR parameters of the T2w sequences.

	3D T2w DRIVE TSE	2D T2w coronal TSE
Acquisition plane	sagittal	coronal
FOV	180 × 180 x 25 mm	180 × 180 x 31 mm
Acquisition voxel	0.6 × 0.6 x 0.6 mm	0.6 × 0.75 x 2.0 mm
Reconstruction voxel	0.3 × 0.3 x 0.3 mm	0.28 × 0.28 x 2.0 mm
Number of slices	83	14
Slice thickness, gap	0.6 mm, -0.3 mm	2 mm, 0.2 mm
Compressed SENSE factor	2.8	no
Scan mode	3D	2D
TSE factor	45	16
Flip angle (degrees)	90	90
TR, TE and TE equivalent	TR 1500 ms TE 148 ms TE 128 ms	TR 2800 ms TE 80 ms
Receiver bandwidth	381 Hz/pixel	525 Hz/pixel
Number of acquisitions NSA	1	2.6
Scan duration	04:03 min	03:55 min

DRIVE sequence and of the coronal 2D T1w GRE sequence are summarized in Tables 1 and 2.

Coronal reconstructions parallel to the pituitary stalk and sagittal reconstructions of images including the pituitary region and the cavernous sinus were obtained both in 0.8 mm and 2 mm slice thickness with an increment of 0.4 mm. Acquisition times and total scan time of the original and of the new pituitary imaging protocol are shown in Table 3.

Concerning the accelerated 3D T1w black blood TSE sequence, a black blood prepulse for blood signal suppression was added. Thus this sequence represents a Compressed SENSE accelerated motion-sensitized driven-equilibrium (MSDE) prepared 3D T1w TSE sequence with an anti-driven equilibrium (ADA) post pulse [7]. Due to the MSDE prepulse this sequence efficiently enables black blood imaging and compared to the MDE-TSE sequence described by Wang et al. [8], an increased T1 contrast is achieved with the ADA post pulse [7].

As described in the introduction the compressed sensing technology used in this study represents a combination of SENSE and compressed sensing, named Compressed SENSE [5,6]. The Compressed SENSE factor and denoising level for the accelerated sequences were defined based on the vendor's implementation.

2.3. Qualitative analysis

Two board-certified neuroradiologists (S.S., 30 years of experience and A.S., 6 years of experience who was additionally assisted by a medical student (T.S.)) assessed the sagittal precontrast and the coronal postcontrast 2D T1w and 3D T1w black blood TSE images independently. Both the images from the 2D and 3D sequence were rated on the 2 mm coronal slices for comparability reasons as described by Kakite et al. [1]. However, the scores from the 3D sequence were also checked on the 0.8 mm slices. For the 3D sequence, the scores from the 2 mm slices always served as the representative value, except when the scores from the 0.8 mm slices were worse than the scores from the 2 mm slices. In such cases, the worse score served as the representative value. For rating of the posterior pituitary on precontrast 2D and 3D T1w images a single midsagittal slice was used.

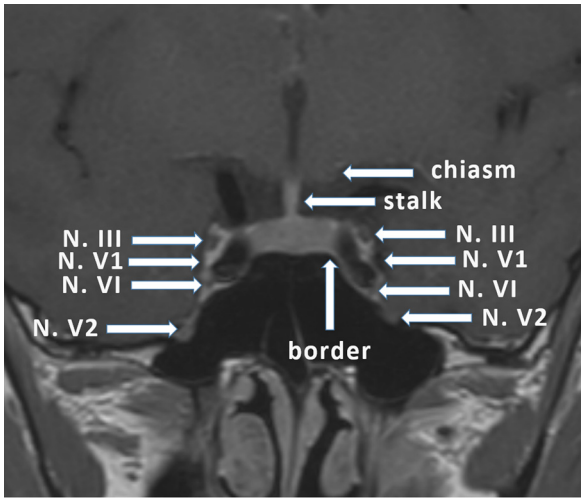

Fig. 1. 2D T1w postcontrast coronal TSE image of a normal pituitary gland with delineation of the cranial nerves N. III (oculomotor nerve), N. V1 (ophthalmic division of trigeminal nerve), N. VI (abducens nerve) and N. V2 (maxillary division of trigeminal nerve) within the cavernous sinus. The pituitary gland with the pituitary stalk and the border between the pituitary gland and the cavernous sinus are depicted.

Images were rated according to a rating scheme partially adopted from Kakite et al. [1].

The following 13 features were evaluated (feature 10 was evaluated on precontrast images, all other features on postcontrast images):

1) The border between the pituitary gland and the cavernous sinus (Figs. 1, 2)
2) The border between the cavernous sinus and the lesion
3) The border between the pituitary gland and the lesion (Figs. 3, 4)
4) The visibility of the ophthalmic nerve (Figs. 1, 2)
5) The visibility of the maxillary nerve (Figs. 1, 2)
6) The visibility of the oculomotor nerve (Figs. 1, 2)
7) The visibility of the optic nerve.
8) The visibility of the optic chiasm (Figs. 1, 2)

Table 3
Scan times of all sequences of the pituitary MR protocol before and after the implementation of Compressed SENSE.

	Previous protocol: Acquisition time of sequences acquired without Compressed SENSE	New protocol: Acquisition time of sequences acquired with Compressed SENSE
2D T1w TSE coronal precontrast	03:11 min	–
2D T1w TSE sagittal precontrast	03:40 min	–
2D dynamic coronal GRE T1w	02:44 min	02:44 min
2D T1w TSE coronal postcontrast	03:11 min	–
2D T1w TSE sagittal postcontrast	03:40 min	–
2D T2w coronal TSE	03:55 min	–
3D T1w black blood TSE transverse precontrast	–	04:35 min
3D T1w black blood TSE transverse postcontrast	–	04:35 min
3D T2w DRIVE sagittal	–	04:03 min
Total scan time	20:21 min	15:57 min
Scan time reduction		21.6%

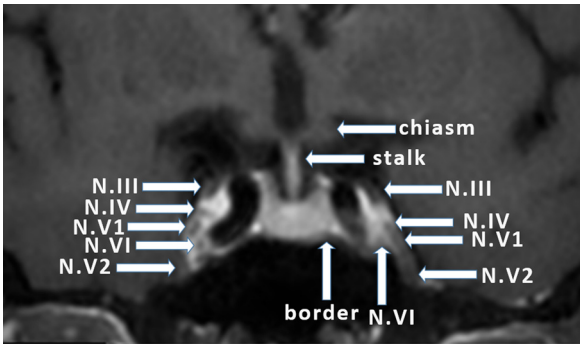

Fig. 2. 3D T1w black blood postcontrast coronal TSE image of a normal pituitary gland with delineation of the cranial nerves N.III (oculomotor nerve), N.IV (trochlear nerve), N.V1 (ophthalmic division of trigeminal nerve), N.VI (abducens nerve) and N.V2 (maxillary division of trigeminal nerve) within the cavernous sinus. The pituitary gland with the pituitary stalk and the border between the pituitary gland and the cavernous sinus are depicted.

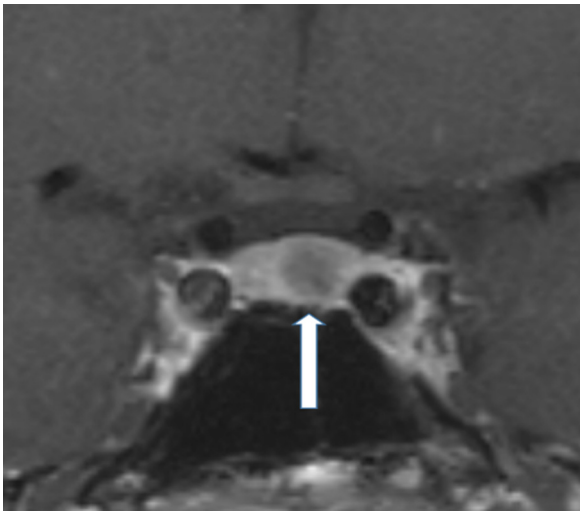

Fig. 3. 2D T1w postcontrast coronal TSE image in a 48y old male patient with slightly hypointense pituitary microadenoma (white arrow) on the left side compared to the normal pituitary gland. The tumor border is slightly blurred. No infiltration into the cavernous sinus on the left side.

Fig. 4. 3D T1w postcontrast coronal TSE image in a 53y old female patient with hypointense pituitary microacenoma (white arrow) on the left side. The tumor border is sharply delineated. No infiltration into the cavernous sinus on the left side.

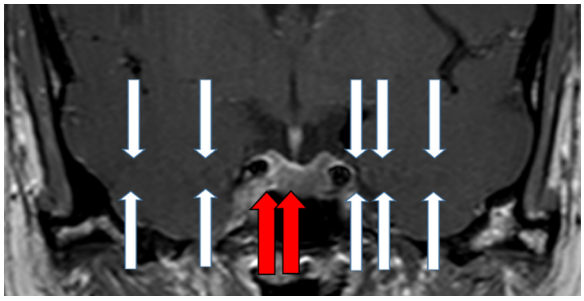

Fig. 5. Pulsation aretefacts (between white arrows) on a postcontrast 2D T1w TSE image. Artefacts present as bandlike iso- to hypointense lines that spread from left to right over the whole image. The pulsation artefacts also expand over the pituitary gland and thus lead to inhomogeneity within the pituitary tissue (marked with red arrows) that impairs the diagnostic image quality. The inhomogeneity could be mistaken as a small microadenoma.

9) The visualization of the pituitary stalk (Figs. 1, 2)
10) The visualization of the posterior pituitary on precontrast T1w images.
11) Presence and severity of susceptibility artefacts.
12) Presence and severity of pulsation artefacts (Fig. 5).
13) Overall image quality.

Oculomotor nerve, ophthalmic and maxillary division of trigeminal nerve were always visible (Figs. 1 and 2). Abducens nerve and trochlear nerve usually could also be delineated, however the presence of hypointense veins within the cavernous sinus made distinction of these small nerves sometimes difficult and therefore these two nerves were not included in the rating despite being depicted in our Figs. 1 and 2.

Features 1 to 10 and 13 were rated according to a 5 point scale with the criteria outlined below: Excellent = 4, Good = 3, Fair = 2, Poor = 1, Non-diagnostic = 0. Features 11 and 12 were evaluated with a 3 point scale: Artefacts are present and are severe enough to impair diagnostic confidence = 2, Artefacts are present but not impairing diagnostic confidence = 1, Artefacts are not present = 0. In case of patients diagnosed with a normal pituitary or with no post-operative residual lesions, features 2 and 3 were not evaluated. For statistical analysis, the mean of the scores from both raters served as the representative value [1].

2.4. Quantitative analysis

Signal to noise ratio (SNR) and contrast to noise ratio (CNR) measurements were performed by drawing region of interests (ROIs) on representative coronal slices of the postcontrast T1w 2D and 3D images, both with 2 mm slice thickness [9]. ROIs were drawn around the solid part of the lesion in case of a pathologic lesion or around the whole pituitary gland in case of a normal pituitary [10] by a board-certified neuroradiologist (S.S., 30 years of experience) [10]. ROI placement was controlled by a second neuroradiologist (A.S., 6 years of experience) and if necessary, ROIs were adjusted until consensus was reached [9,11].

SNR was calculated by dividing the average signal intensity of the ROI placed on the tissue (SI_{tissue}) of interest by the standard deviation of the tissue ROI (SD_{tissue}) [9]. The pituitary (tissue1) – white matter (tissue2) CNR was calculated according to the following formula:

$$\left| \frac{(SI_{tissue1} - SI_{tissue2})}{\sqrt{(SD_{tissue1}{}^2 + SD_{tissue2}{}^2)}} \right|$$

SNR and CNR formulas utilized can be used for accelerated sparse images as in the case of images acquired with compressed sensing technology [9,11].

Table 4
Rating scores of qualitative and quantitative image quality features. The 3D T1w black blood TSE sequence outperformed the 2D T1w TSE sequence in terms of "presence and severity of pulsation artefacts "and" overall image quality" (marked in bold letters). Significant p values were underlined.

	2D T1w TSE Mean ± SD; median; IQR	3D T1w black blood TSE with Compressed SENSE Mean ± SD; median; IQR	Intraclass Correlation Coefficient (ICC)	p value
Overall image quality	3.27 ± 0.65; 3.00; [3.00;4.00]	3.64 ± 0.49; 4.00; [3.00;4.00]	0.8	0.04
Presence and severity of pulsation artefacts	1.07 ± 0.70; 1.00; [1.00;1.63]	0.04 ± 0.19; 0.00; [0.00;0.00]	0.97	< 0.001
Border between the pituitary gland and the cavernous sinus	3.91 ± 0.24; 4.00; [4.00;4.00]	3.71 ± 0.52; 4.00; [3.50;4.00]	0.77	0.29
Border between the cavernous sinus and the lesion	3.78 ± 0.46; 4.00; [4.00;4.00]	3.68 ± 0.61; 4.00; [3.50;4.00]	0.78	0.72
Border between the pituitary gland and the lesion	3.44 ± 0.76; 4.00; [3.00;4.00]	3.35 ± 0.68; 3.50; [2.50;4.00]	0.71	0.53
Visibility of the Ophthalmic nerve	3.04 ± 0.72; 3.00; [2.50;3.50]	2.71 ± 0.64; 2.50; [2.50;3.00]	0.57	0.11
Visibility of the Maxillary nerve	3.04 ± 0.61; 3.00; [2.88;3.50]	2.71 ± 0.77; 2.75; [2.38;3.50]	0.62	0.17
Visibility of the Oculomotor nerve	3.84 ± 0.33; 4.00; [4.00;4.00]	3.77 ± 0.44; 4.00; [3.88;4.00]	0.7	0.75
Visibility of the Optic nerve	4.00 ± 0.00; 4.00; [4.00;4.00]	3.96 ± 0.19; 4.00; [4.00;4.00]	1	0.83
Visibility of the Optic Chiasm	4.00 ± 0.00; 4.00; [4.00;4.00]	3.95 ± 0.28; 4.00; [4.00;4.00]	0.8	0.83
Visualization of the Pituitary stalk	3.91 ± 0.27; 4.00; [4.00;4.00]	3.96 ± 0.19; 4.00; [4.00;4.00]	0.85	0.66
Visualization of the posterior pituitary on non-contrast enhanced T1w images	3.48 ± 0.70; 4.00; [3.00;4.00]	3.81 ± 0.46; 4.00; [4.00;4.00]	0.79	0.12
Presence and severity of susceptibility artefacts	0.13 ± 0.35; 0.00; [0.00;0.00]	0.20 ± 0.39; 0.00; [0.00;0.00]	0.77	0.63
SNR	11.69 ± 4.86; 11.46; [8.34;15.18]	10.48 ± 4.92; 9.89; [7.24;12.48]	–	0.204
CNR	4.10 ± 1.83; 4.12; [3.43;5.49]	3.22 ± 1.73; 2.96; [2.03;4.64]	–	0.07

2.5. Statistical analysis

The interreader agreement for the qualitative scores was assessed by calculating the intraclass correlation coefficient (ICC) [12]. An ICC of 0.75 to 1.00 was deemed as excellent, 0.60 to 0.74 good, 0.40 to 0.59 fair, and less than 0.4 as poor agreement [12]. Scores from the qualitative and quantitative analysis were compared with the exact Wilcoxon rank sum test. P values < 0.05 were considered significant.

3. Results

A detailed overview of the scores from the qualitative and quantitative analysis (SNR, CNR) is given in Table 4. In brief, the interreader agreement ranged from fair (visibility of the ophthalmic nerve, ICC = 0.57) to excellent (presence and severity of pulsation artefacts, ICC = 0.97). Generally, larger structures exhibited better interreader agreement (e.g. optic nerve or chiasm) than smaller structures (e.g. maxillary or ophthalmic nerve). There were no significant differences in any qualitative features evaluated except for the features "presence and severity of pulsation artefacts" (median: 0 versus 1, $p < 0.001$) and "overall image quality" (median: 4 versus 3, $p = 0.04$), with the 3D sequence outperforming the 2D sequence. As for the quantitative features, there were no significant changes in SNR and CNR.

By replacing the 2D T1w pre- and postcontrast sequences with the 3D T1w black blood TSE pre- and postcontrast sequences (Table 3), a scan time reduction of 33.1% (13:42 min versus 09:10 min) was achieved. The scan time of the whole MR protocol (including the T2w sequences) could be reduced from 20:23 min to 15:57 min thus leading to a time saving of 04:24 min (21.6%).

4. Discussion

In this study we compared image quality between a 2D T1w TSE sequence and a Compressed SENSE accelerated 3D T1w black blood TSE sequence in pre- and postcontrast imaging of the pituitary and assessed the possible scan time reduction. 13 qualitative image quality features were rated, whereby 12 features were rated on postcontrast and 1 feature on precontrast images. Images from the 3D T1w black blood TSE sequence were given equal or even better image quality scores in comparison to images from the 2D T1w TSE sequence. Specifically, the presence and severity of pulsation artefacts was significantly reduced on images acquired with the Compressed SENSE accelerated 3D sequence and the overall image quality was deemed superior on 3D images. As for quantitative features, no significant difference in SNR and CNR measurements obtained on identical slice thickness in images acquired with 2D and 3D TSE technique was found. Ultimately, a scan time reduction of 33.1% was achieved by replacing 2D T1w TSE sequences with the Compressed SENSE accelerated 3D T1w black blood TSE sequences.

In a clinical setting not only the scan duration but also the spatial resolution of the images is important. This is especially true for small pathologies occurring frequently in the pituitary and parasellar regions that can go undetected on standard 2D sequences with a slice thickness of 2–3 mm. The use of 3D sequences in high resolution technique allows the imaging of very small pathologies in the submillimeter range and is thus preferable [1,3]. Our results indicate that 3D T1w sequences accelerated with Compressed SENSE outperform conventional 2D sequences in pituitary imaging in terms of image quality and thus are desirable alternatives that can be used clinically.

Comparable or even better image quality together with reduced acquisition time obtained in sequences acquired with compressed sensing technology and with or without 3D technique was already demonstrated in several anatomical regions [13–23] as for example in hepatobiliary imaging [17], in lumbar spine imaging [18], in intracranial vessel and brain imaging in general [19,21,23] and for different MR sequences as for example for the double inversion recovery (DIR) sequence used for delineation of demyelinating lesions in multiple sclerosis [20]. Specifically a large study [23] assessing several compressed sensing accelerated sequences used routinely in brain imaging has found that the introduction of compressed sensing technology saved considerable imaging time while allowing to increase spatial resolution without compromising image quality. Two neuroradiologists rated images with a 5-point linkert scale whilst recording acquisition times for all sequences. The median scan time reduction was 29.3% and the median voxel size could be reduced by 10.5%. As for the image quality, the compressed sensing accelerated 3D Fluid-attenuated Inversion Recovery (FLAIR), 3D T2 and axial T2* sequences outperformed the non-accelerated images while for the other sequences evaluated (3D DIR, 3D T1, 3D T1 + gadoteric acid, axial T2, axial FLAIR and 3D arterial time-of-flight MR angiography (art. TOF)) no statistical difference in image quality was noted.

Furthermore, a recent study focusing specifically on the performance of a compressed sensing accelerated 3D TOF sequence [21] found the accelerated sequence to outperform a conventional sequence in terms of image quality, blurring and the visualization of the external carotid arteries whilst maintaining diagnostic performance of

intracranial arteries. Rating was performed by three radiologists on 49 consecutive patients who were scanned with both the accelerated and non-accelerated TOF sequence [21].

Thus, compressed sensing technology seems to be of great value, especially in brain imaging, as it provides the possibility of reducing scan times whilst maintaining image quality.

Besides the study of Mönch et al. [23] who reported a median scan time reduction of 29.3% in brain imaging, another recent study [5] has shown that the application of compressed sensing technology to MR protocols enables a scan time reduction ranging from 14% (in wrist imaging) to 41% (in lumbar spine imaging). Scan time reductions are of interest to clinical institutions as they enable an increase in patient examinations, which ultimately has some financial significance. Moreover, patients also appreciate the increased comfort stemming from shorter MR examination times [5]. We observed similar scan time reductions by redesigning our pituitary MR protocol.

It has been shown, however, that images acquired with compressed sensing technology may present with artefacts in brain imaging [6]. Besides motion artefacts appearing in phase direction as semi-circular rings, special artefacts occurring specifically on images acquired with compressed sensing have been observed: 1.) The wax-layer artefact, where images appear as if they are covered by a thin inhomogeneous layer of wax. 2.) The streaky-linear artefact wherein images are covered with streaks (long or short lines) in horizontal of oblique orientation. 3.) The starry-sky artefact where images seem to appear grainy and slightly pixelated. These artefacts presented mostly on 3D FLAIR and 3D T1 m-Dixon Turbo Field Echo (TFE) images, yet only rarely (or never) on images originating from other sequences (such as the 3D DIR sequence). Eichinger et al. [20] evaluated the utility of compressed sensing in 3D DIR imaging of patients with multiple sclerosis and even found the accelerated 3D DIR sequence to be considerably less prone to artefacts than the conventional sequence. Furthermore Mönch et al. [23] also described only few mild artefacts in their compressed sensing brain imaging study. Similar to these reports our results also indicate that the Compressed SENSE accelerated 3D T1w black blood TSE sequence presented with less artefacts than the conventional 2D TSE sequence. Specifically, the presence and severity of pulsation artefacts (Fig. 5) was significantly reduced on images acquired with the Compressed SENSE accelerated 3D sequence. Even though we did not separately evaluate the influence of Compressed SENSE and the MSDE prepulse on the reduction of pulsation artefacts in the 3D T1w sequence, one can assume that the reduction of these artefacts are mainly caused by the black blood prepulse and not by Compressed SENSE. This reduction of pulsation artefacts may have ultimately also contributed to the improved rating of the overall image quality on the 3D images compared to the 2D sequences.

Finally, our study has some limitations:

Firstly, the main limitation of our study is the retrospective study design with all its inherent limitations [11]. We did not perform an intra-individual comparison of sequences, which would have greatly increased the scientific merit of the study and would have boosted confidence in the data. However, it has to be noted, that we mostly evaluated postcontrast T1w sequences and as such one would have had to administer contrast media twice in each patient for optimal comparison of the sequences, as the timing of the sequence acquisition after contrast media administration is essential. Alternatively, also given a prospective study design, one could have divided the patients into two groups whereby the 3D T1w sequence would have been acquired first in the first group followed by the 2D T1w sequence; For the second group the order of sequence acquisition could have been reversed thus minimizing possible bias due to the postcontrast enhancement curve of the pituitary glands and possible lesions [24]. Therefore we highly recommend checking the reproducibility of our results in a future prospective study. Secondly, as outlined previously, the black blood prepulse was only added in the 3D sequences. Thus the image quality feature "Presence and severity of pulsation artefacts" cannot be considered a direct comparison. Furthermore, the sample size was somewhat limited, but in the typical range for clinical pilot studies of this kind [1,9]. Next, we are aware that there may be several formulas to calculate CNR and SNR on sparse images. We selected two formulas that were recently utilized in similar studies [9,11]. However, different formulas have been applied as well in the literature and may yield slightly different results [21].

5. Conclusion and outlook

3D T1w black blood TSE sequences accelerated with Compressed SENSE outperform conventional 2D T1w TSE sequences in pituitary MR imaging as scan times can be reduced while image quality is maintained or even improved. Thus, Compressed SENSE accelerated 3D T1w blood TSE sequences represent a viable option for clinical use in pituitary imaging. For the future, it may be interesting to compare the performance of accelerated 3D T1w black blood TSE sequences to other sequences, such as 3D T1w GRE sequences.

Author contributions

TS, ES, ASB, SS and MW designed the study and interpreted the results. TS, SS, CB, BE, LVS, MW, AS and AN performed the experiments. ASB and TS analyzed the data. TS, SS, ASB and MW wrote the paper. CB provided technical advice. All coauthors contributed constructively to the manuscript.

Funding

No funding was received for this study.

Data statement

Data is available upon enquiry to the corresponding author.

Declaration of Competing Interest

MW is a part time employee of Philips Healthcare Switzerland. The other authors declare no conflict of interest.

References

[1] S. Kakite, S. Fujii, M. Kurosaki, Y. Kanasaki, E. Matsusue, T. Kaminou, T. Ogawa, Three-dimensional gradient echo versus spin echo sequence in contrast-enhanced imaging of the pituitary gland at 3T, Eur. J. Radiol. 79 (2011) 108–112, https://doi.org/10.1016/j.ejrad.2009.12.036.

[2] A.S. Arbab, 3D gradient echo sequence provides better images in contrastenhanced imaging of the pituitary gland at 3T, Imaging Med. 2 (2010) 129–130.

[3] R.J. Lien, I. Corcuera-Solano, P.S. Pawha, T.P. Naidich, L.N. Tanenbaum, Three-Tesla imaging of the pituitary and parasellar region: T1-weighted 3-dimensional fast spin echo cube outperforms conventional 2-dimensional magnetic resonance imaging, J. Comput. Assist. Tomogr. 39 (2015) 329–333, https://doi.org/10.1097/RCT.0000000000000214.

[4] L. Geerts-Ossevoort, E. de Weerdt, A. Duijndam, et al., Compressed SENSE. Speed Done Right. Every Time, May16 Philips® Healthcare, Netherlands, 2018Https://philipsproductcontent.blob.core.windows.net/assets/20180109/619119731f2a42c4acd4a863008a46c7.pdf..

[5] E. Sartoretti, T. Sartoretti, C. Binkert, A. Najafi, Á. Schwenk, et al., Reduction of procedure times in routine clinical practice with Compressed SENSE magnetic resonance imaging technique, PLoS One 14 (4) (2019) e0214887, https://doi.org/10.1371/journal.pone.0214887.

[6] T. Sartoretti, C. Reischauer, E. Sartoretti, C. Binkert, A. Najafi, S. Sartoretti-Schefer, Common artefacts encountered on images acquired with combined compressed sensing and SENSE, Insights Imaging 9 (2018) 1107–1115, https://doi.org/10.1007/s13244-018-0668-4.

[7] M. Yoneyama, M. Nakamura, T. Takahara, A. Takemura, M. Obara, T. Tabuchi, S. Tatsuno, S. Sawano, Improvement of T1 contrast in whole-brain black-blood imaging using motion-sensitized driven-equilibrium prepared 3D turbo spin echo (3D MSDE-TSE), Magn. Reson. Med. Sci. 13 (2014) 61–65, https://doi.org/10.2463/mrms.2013-0047.

[8] J. Wang, V.L. Yarnykh, C. Yuan, Enhanced image quality in black-blood MRI using the improved motion-sensitized driven-equilibrium (iMSDE) sequence, J. Magn. Reson. Imaging 31 (2010) 1256–1263, https://doi.org/10.1002/jmri.22149.

[9] S.H. Lee, Y.H. Lee, J.S. Suh, Accelerating knee MR imaging: compressed sensing in isotropic three-dimensional fast spin-echo sequence, Magn. Reson. Imaging 46 (2018) 90–97, https://doi.org/10.1016/j.mri.2017.10.018.

[10] L. Yiping, L. Hui, Z. Kun, G. Daoying, Y. Bo, Diffusion-weighted imaging of the sellar region: a comparison study of BLADE and single-shot echo planar imaging sequences, Eur. J. Radiol. 83 (2014) 1239–1244, https://doi.org/10.1016/j.ejrad.2014.03.011.

[11] F.F. Altahawi, K.J. Blount, N.P. Morley, E. Raithel, I.M. Omar, Comparing an accelerated 3D fast spin-echo sequence (CS-SPACE) for knee 3-T magnetic resonance imaging with traditional 3D fast spin-echo (SPACE) and routine 2D sequences, Skeletal Radiol. 46 (2017) 7–15.

[12] D. Stocker, A. Manoliu, A.S. Becker, B.K. Barth, D. Nanz, M. Klarhöfer, O.F. Donati, Image quality and geometric distortion of modern diffusion-weighted imaging sequences in magnetic resonance imaging of the prostate, Invest. Radiol. 53 (2018) 200–206, https://doi.org/10.1097/RLI.0000000000000429.

[13] F.K. Lohöfer, G.A. Kaissis, M. Rasper, C. Katemann, A. Hock, J.M. Peeters, C. Schlag, E.J. Rummeny, D. Karampinos, R.F. Braren, Magnetic resonance cholangiopancreatography at 3 Tesla: image quality comparison between 3D compressed sensing and 2D single-shot acquisitions, Eur. J. Radiol. 115 (2019) 53–58, https://doi.org/10.1016/j.ejrad.2019.04.002.

[14] J. Yi, Y.H. Lee, S. Hahn, S.S. Albakheet, H.T. Song, J.S. Suh, Fast isotropic volumetric magnetic resonance imaging of the ankle: acceleration of the three-dimensional fast spin echo sequence using compressed sensing combined with parallel imaging, Eur. J. Radiol. 112 (2019) 52–58, https://doi.org/10.1016/j.ejrad.2019.01.009.

[15] M. Nakamura, T. Kido, T. Kido, K. Watanabe, M. Schmidt, C. Forman, T. Mochizuki, Non-contrast compressed sensing whole-heart coronary magnetic resonance angiography at 3T: a comparison with conventional imaging, Eur. J. Radiol. 104 (2018) 43–48, https://doi.org/10.1016/j.ejrad.2018.04.025.

[16] B. Henninger, E. Raithel, C. Kranewitter, M. Steurer, W. Jaschke, C. Kremser, Evaluation of an accelerated 3D SPACE sequence with compressed sensing and free-stop scan mode for imaging of the knee, Eur. J. Radiol. 102 (2018) 74–82, https://doi.org/10.1016/j.ejrad.2018.03.001.

[17] J.G. Nam, J.M. Lee, S.M. Lee, H.J. Kang, E.S. Lee, B.Y. Hur, J.H. Yoon, E. Kim, M. Doneva, High acceleration three-dimensional T1-Weighted dual echo dixon hepatobiliary phase imaging using compressed sensing-sensitivity encoding: comparison of image quality and solid lesion detectability with the standard T1-Weighted sequence, Korean J. Radiol. 20 (2019) 438–448, https://doi.org/10.3348/kjr.2018.0310.

[18] K. Morita, T. Nakaura, N. Maruyama, Y. Iyama, S. Oda, D. Utsunomiya, T. Namimoto, M. Kitajima, M. Yoneyama, Y. Yamashita, Hybrid of compressed sensing and parallel imaging applied to three-dimensional isotropic T2-weighted Turbo spin-echo MR imaging of the lumbar spine, Magn. Reson. Med. Sci. (2019), https://doi.org/10.2463/mrms.mp.2018-0132.

[19] C.H. Suh, S.C. Jung, H.B. Lee, S.J. Cho, High-resolution magnetic resonance imaging using compressed sensing for intracranial and extracranial arteries: comparison with conventional parallel imaging, Korean J. Radiol. 20 (2019) 487–497, https://doi.org/10.3348/kjr.2018.0424.

[20] P. Eichinger, A. Hock, S. Schön, C. Preibisch, J.S. Kirschke, M. Mühlau, C. Zimmer, B. Wiestler, Acceleration of double inversion recovery sequences in multiple sclerosis with compressed sensing, Invest. Radiol. 54 (2019) 319–324, https://doi.org/10.1097/RLI.0000000000000550.

[21] Z. Lin, X. Zhang, L. Guo, K. Wang, Y. Jiang, X. Hu, Y. Huang, J. Wei, S. Ma, Y. Liu, L. Zhu, Z. Zhuo, J. Liu, X. Wang, Clinical feasibility study of 3D intracranial magnetic resonance angiography using compressed sensing, J. Magn. Reson. Imaging (2019), https://doi.org/10.1002/jmri.26752.

[22] A.S. Gersing, J. Bodden, J. Neumann, M.N. Diefenbach, S. Kronthaler, D. Pfeiffer, C. Knebel, T. Baum, B.J. Schwaiger, A. Hock, E.J. Rummeny, K. Woertler, D.C. Karampinos, Accelerating anatomical 2D turbo spin echo imaging of the ankle using compressed sensing, Eur. J. Radiol. (2019), https://doi.org/10.1016/j.ejrad.2019.06.006.

[23] S. Mönch, N. Sollmann, A. Hock, C. Zimmer, J.S. Kirschke, D.M. Hedderich, Magnetic resonance imaging of the brain using compressed sensing - quality assessment in daily clinical routine, Clin. Neuroradiol. (2019), https://doi.org/10.1007/s00062-019-00789-x.

[24] Magnaldi S, Frezza F, Longo R, Ukmar M, Razavi IS, Pozzi-Mucelli RS. Assessment of pituitary microadenomas: comparison between 2D and 3D MR sequences, Magn. Reson. Imaging 15 (1) (1997) 21–27.